Modelling And Optimisation Of A Vaporiser For Inhalation Drug Therapy

B. de Heij , B. van der Schoot, N. F. de Rooij, Hu Bo* and J. Hess*
IMT, University of Neuchâtel, P.O.box 3, 2007 Neuchâtel, Switzerland
(tel +41 32 7205 261 fax +41 32 7205 711) Bas.deHeij@imt.unine.ch
* Microflow Engineering SA

ABSTRACT

We present a piezo-electrically driven droplet generator with a large number of nozzles working in parallel and operating in the Drop On Demand mode. This device is build as part of a system for Inhalation Drug Therapy. Details of modelling and optimisation of this device are explained. The operation of the device is resonance dependent. To arrive at a higher throughput and a more reliable operation, modeshape analysis has been performed. Finally an improved design was proposed which uses modeshape targeting. Final results are a fast prototyping platform and a set of design rules.

keywords: vaporiser, modeshapes, design rules, monodispersive drop generation.

INTRODUCTION

General

Asthma is one of the fastest growing diseases in the industrialised parts of the world. Mostly asthma is treated with Inhalation Drug Therapy (IDT). A vapour of medicine is inhaled and transported by the air stream to the lung-sacs where it has its therapeutic effect. Commonly used Metered Dose Inhalers (MDI's) generate a vapour, from a spray can, with a fixed total volume and a certain droplet size distribution. Only droplets within a small diameter range will be able to penetrate deep into the lungs [1]. Anything outside this size range will be none effective and can cause side effects. Ideally the inhalation vapour should be mono-dispersive.

It is possible to generate droplets of a very narrow size distribution by using a mist generator based on Drop On Demand ink-jet techniques [2,3]. The size of droplets generated in this way is defined by the size of the nozzle used. Recent developments in Deep Reactive Ion Etching (DRIE) make it possible to etch nozzles in the appropriate size range for an IDT vaporiser. By using an electrically actuated device it also possible to adapt the flow of medicine to the measured actual breath flow.

The device

The device (see Fig 1,2.) consists of a fluid chamber with on one side a piezo disk for actuation and nozzles (up to 1300) on the other side made in silicon micro-technology. With

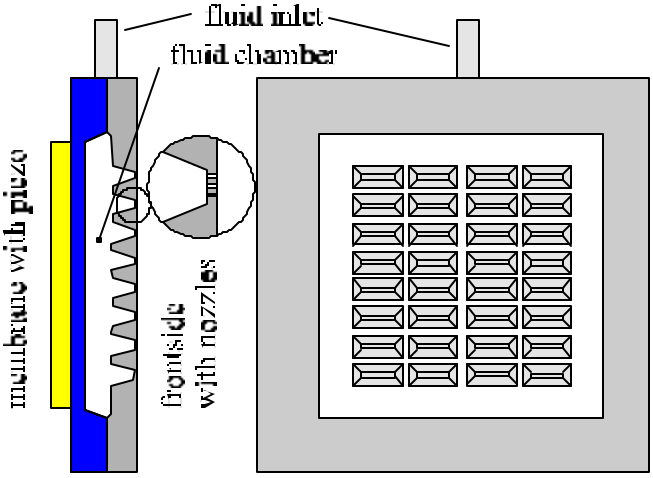

Fig. 1. Principle layout of the device.

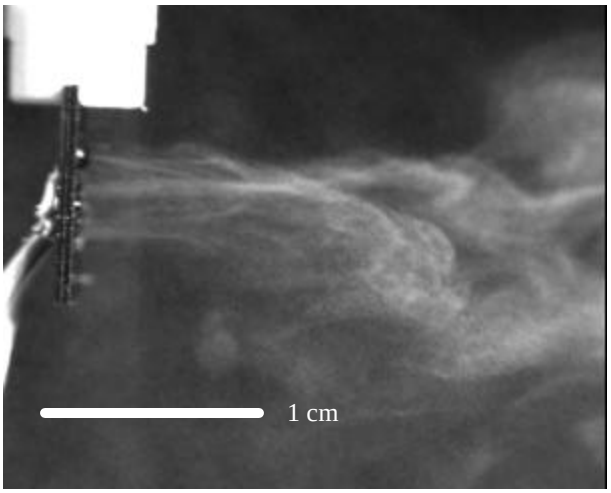

Fig. 2. The device in action

the actuation of the piezo a pressure wave travels towards the front side and causes liquid to exit through the nozzle. With enough kinetic energy the liquid breaks off the nozzle and forms a small droplet. It is necessary to use a high actuation frequency to get high enough kinetic energy to break the surface tension of the liquid. At these high frequencies, the device no longer vibrates in its basic (first) mode. A complex pattern of extremes *(standing waves patterns)* will exist. Secondly it is necessary to use such a high frequency to get a high enough flow;

$Q = (\frac{1}{6} \cdot p \cdot d^3) \cdot f \cdot n$. In which *d* is the droplet diameter, *f* the actuation frequency and *n* the number of holes. Typical values of 5µm droplet diameter 250kHz actuation frequency and a desired flow of 20µl/s give an *n* of 1222. Geometrically this is about the upper limit of nozzles that can be placed on the front plate of a $1cm^2$ device.

OPTIMISATION PROCEDURE

Identification

The device only ejects droplets at certain frequencies (frequency ranges). This indicates that operation is resonance dependent. Measurement of the impedance curve (on the piezo) readily confirms this (see Fig. 3) At the resonance the device exhibits a standing wave pattern which can be easily observed with a Michelson interferometer. Here the device is used as one of the mirrors (see Fig 4). An exposure time, on the camera, longer then one vibration period will show the moving parts as grey areas, nodal lines will show the basic interference pattern (see Fig. 5). At the resonance only certain parts of the device vibrate and only the nozzles at these parts will be able to eject droplets. Nozzles that receive insufficient pressure can cause large liquid droplets on the front plate that eventually block other nozzles.

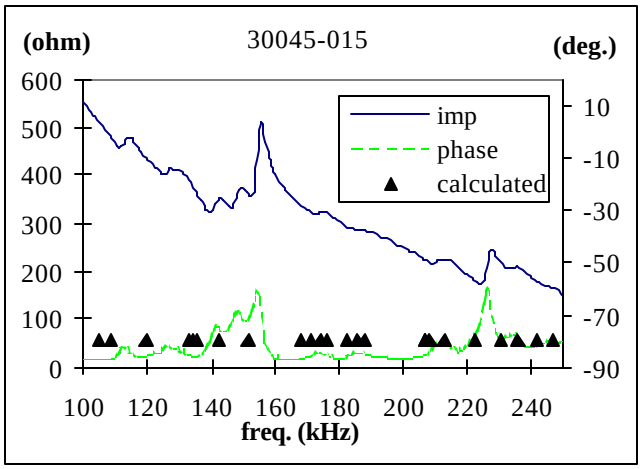

Fig. 3. The impedance curve of a particular device with calculated resonance frequencies. The strength of each resonance and the mixing of resonance's can also be seen.

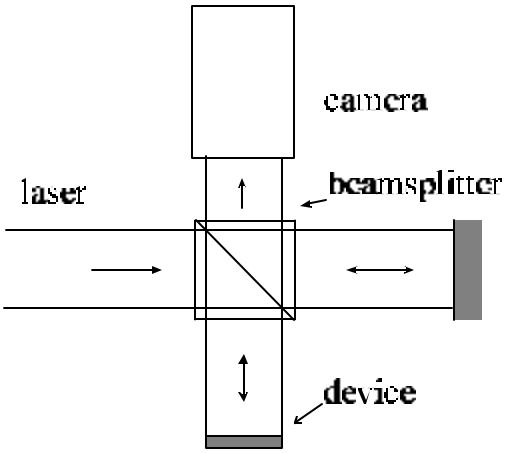

Fig. 4. The interferometer set-up

Modelling

Feeding the device's geometry in the FEM solver produced the same resonance modes. Basic differences from the calculated resonance frequencies and reality come from;

- discretisation error; finite number of elements in the mesh
- geometrical differences; real device has production tolerances
- real boundary conditions are not as rigid as in the calculation.

Calculated resonance frequencies are within 10% of the experimental values thus validating the calculations.

The backside of the piezo is not accessible for interferometer observation. The simulation result showed however that the nodal pattern on the back side was very different from the front side. The combination of the front and backside motion determine the available pressure at the nozzle. Maximising 1) the available pressure i.e. the amplitude and 2) the area where this pressure is available are the optimisation criteria.

Optimisation

The flow resistance in the nozzle is of major importance for the drop ejection and thus most of the shape of the front plate is fixed. The freedom left for the optimisation are size and thickness of the membrane and piezo. Also the shape of the membrane can be changed. Secondly with a known modeshape the nozzles should be placed on the extremes. It is important to keep the manufacturability in mind with every optimisation step.

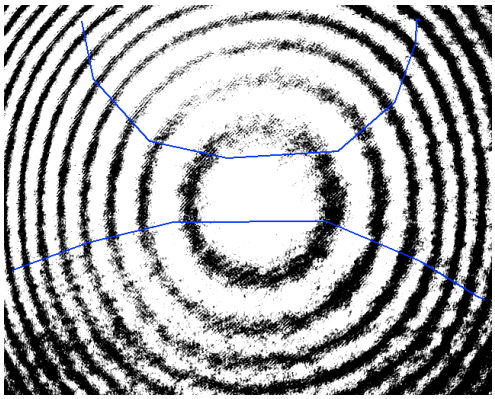

Fig. 5. Example of an interferogram. The moving parts are grey while the nodal lines show a clean interference pattern.

RESULTS

Building and validating model

We are interested in higher order modes of the device so convergence and accuracy of the FEM model are not that trivial. Moreover the device itself is of a complex shape. These two factors demand a high number of elements in the mesh. Calculation time and available computer storage are limiting factors that demand a low number of element. The first run showed that we needed at least 40 modes to get through the frequency range of interest. Bringing back the model from 3000, 27-node elements to 2000, 8-node elements lost some accuracy but gained calculation time (see Table I).

Table I: Comparison of 27 and 8 node elements

element type	elements	modes requested	calculation time (h)	storage* (Gb)
27 node	3000	40	9	2
8 node	2000	40	0.75	0.5

* during calculation

A second method to limit calculation time is by replacing complex parts of the device with 'preconditioned' simpler parts. For instance the complex structure of the front plate can be replaced by just one slab (cf. Fig. 6) with an effective E' and ρ'. Here the formula from Timoshenko [4] for a fully clamped membrane is used.

$$f_n = \tfrac{1}{2}\pi \frac{\lambda_n}{a^2}\cdot\sqrt{\frac{D}{\rho h}}$$

$$D = \frac{Eh^3}{12(1-\nu^2)} \qquad (1)$$

f_n: Modal frequency λ_n: Constant a: width h: thickness.
With the constant λ taken from [5]. The effective properties were deduced from the calculated resonance frequencies of the complex parts. For the 27-node elements this proved useful but the method is certainly not improving the accuracy and flexibility.

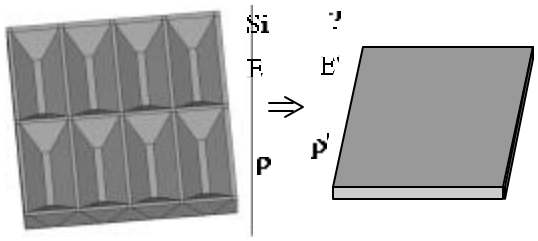

Fig. 6. The replacement to minimise calculation time

The interferometer was the main instrument to compare simulation results with reality. Two effects turned up: not all modes are equally strong present and due to a finite quality factor (Q-factor) some modes appear simultaneously. Both effects can be seen also in the impedance curve of the device (see Fig. 3) Strong resonanses have large phase shifts. The mixing of modes can be seen in areas where there are several peaks appearing together without a clear spacing. For the functioning of the device only modes that are strong and clearly separated from the others are of interest.

In reality the device functions with the chamber (Fig 1.) filled with liquid. This presumably changes the mechanical behaviour due to a changed coupling between the front and back side. From the measurement of impedance curves of several devices with and without water in the chamber it was found that there is little influence from the liquid i.e. the curves did not change shape but only shifted some 2% in frequency. This indicated that the two sides are tightly coupled through the outside rim. Leaving the water out makes the modelling considerably easier.

Varying the membrane dimensions.

The frequency of the first mode on the back and front side differ by a factor of 1.5. From eq. 1 it can already be seen that just the thickness of a membrane is of linear influence on the frequency. For a coupled system this influence of the membrane thickness will be even lower. The membrane should be almost a full wafer (400µm) thick to arrive at the ideal point. This would totally diminish the amplitude of the vibration. Conclusion is that by only varying the membrane thickness the optimal design can not be reached. Changing the membrane size while keeping the total device size constant showed the importance of a tight coupling between the two sides. With a wider rim the induced amplitude is much higher. When the piezo was the same size as the membrane also an amplitude maximum was found.

Varying the membrane shape

Objects that are geometrically the same will have the same resonance frequencies. This led to the design with two similar silicon structures as back and front side. The only anti-symmetry left as is the piezo disk on the backside. (see Fig. 7). This design immediately gave better results, first modal frequencies from back and front only differ by a factor of 1.2. Anti-symmetrically changing the chamber depth can bring the two modes together. Even when these first modes do not appear together there still can be some interesting modes at higher frequencies. In these case a mode on one side can induce a similar vibration on the other side. These cases are actually more interesting because they will have a higher stability in practical samples. These designs were also build to verify simulation results. These were the first devices to work at very specific frequencies,

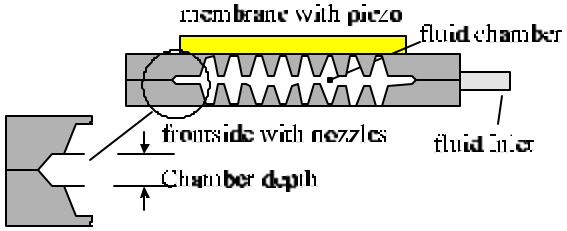

Fig. 7. The new design with similar back and front side.

indicating that only certain resonance modes worked, exactly as predicted by the simulations.

Placement of the nozzles

The ejection nozzles should be placed there where there is sufficient amplitude for droplet ejection, hence close to the extremes of the mode. Nozzles that are not properly placed can cause large droplets on the front plate which in turn can block other holes. From previous simulation results three modes were taken and further analysed. Several designs were proposed that each targeted a particular mode. Two of these are shown in Fig. 8 with their targeted mode in resp Fig. 9 and 10.

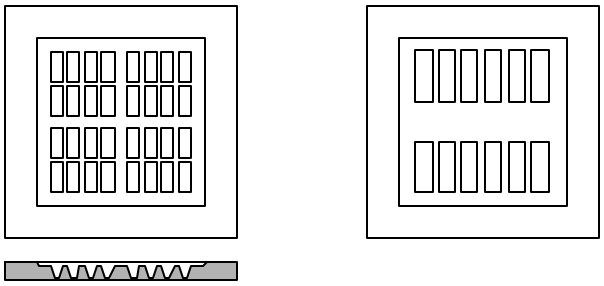

Fig. 8. Two of the mode targeted layouts

Boundary conditions

The device needs some connection with the macro world. These connections should not hinder the vibration of the device. Taking only a small hole in the middle of one side gave the smallest influences. Fixing one whole side clearly damped out a number of modes. In practical samples this was also clearly visible, up to the point were certain designs stopped functioning.

CONCLUSION/DISCUSSION

FEM modeshape analysis proved to be a valuable tool in this case. The comparison with real samples was crucial to validate the model. The final result is a fast prototyping tool that can validate design variation. This tool can also be used to set production tolerances.

By making use of the resonance modes and new production techniques (DRIE) we were for the first time able to make a drop on demand device working in this size range. Due to its construction it is insensitive to the fluid used, unlike other ink-jet devices.

ACKNOWLEDGEMENTS

This project is financed by the Swiss priority programme MINAST (proj. nr. 1.06.2) and done in co-operation with Microflow Engineering SA CH-2007 Neuchâtel. jhess@microflow.ch

REFERENCES

[1] W. Hofmann, 'Lung morphometry and particle transport and deposition overview of existing models', in; 'Aerosol inhalation: Resent research frontiers' ed. J.C.M. Marijnissen, Kluwer Dordrecht 1996

[2] W.G. Hawkins, 'A fully integrated Silicon-Based 40V Thermal ink jet IC'; M.electr.Eng 1992 (19) 165-170

[3] M- Datta, 'Fabrication of an array of precision nozzles by through mask electrochemical micromachining.' J.Electrochem.Soc. 1995 (142) 3801-3805

[4] Timoshenko S. 'Vibration problems in engineering', fourth edition 1974 J. Wiley & Sons. NY.

[5] Warburton G.B. 'The vibration of rectangular plates', Proc. Inst. Mech. Eng. Ser A 1954 (168) 371-384

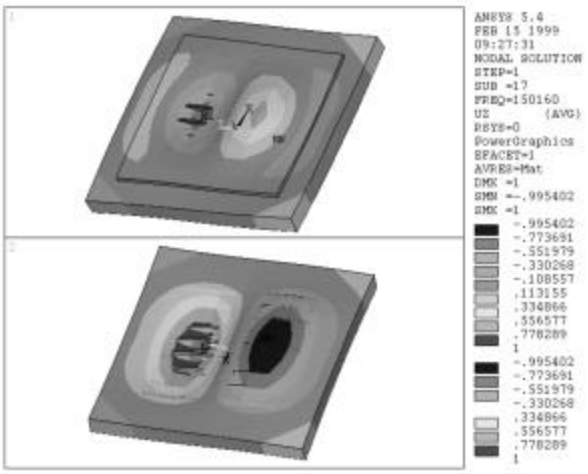

Fig. 9. Simulated result of the right-hand design in Fig. 8

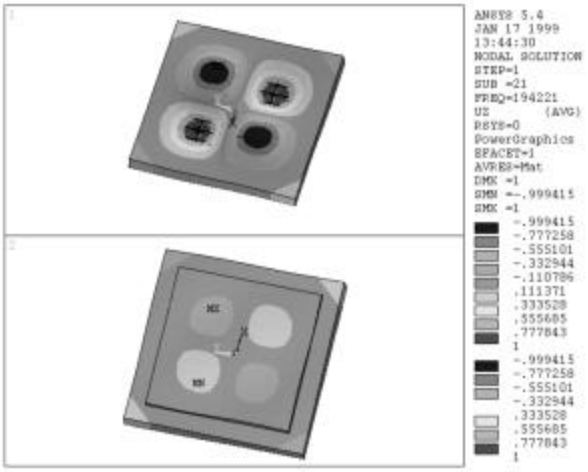

Fig. 10. Simulation result of the left-hand design in Fig. 8